Imaging and Radiation Research (2019) Volume 2 Issue 1
doi:10.24294/irr.v2i1.1717

ORIGINAL RESEARCH ARTICLE

Radiation dose and image quality in a pediatric interventional cardiology team

Carlos Ubeda[1]*, Patricia Miranda[2], Dandaro Dalmazzo[3]

[1] Laboratorio de Dosimetría Personal, Centro de Estudios en Ciencias Radiológicas (CECRAD), Facultad de Ciencias de la Salud, UTA. Arica, Chile. E-mail: carlos.ubeda.uta@gmail.com*

[2] Hospital Luis Calvo Mackenna. Santiago, Chile.

[3] Instituto Nacional del Cáncer y Facultad de Salud y Odontología, Universidad Diego Portales, Santiago, Chile.

ABSTRACT

The optimized methodology and results of the new characterization in terms of dose and image quality of the X-ray system used in the main pediatric hemodynamics service in Chile are presented. In addition, scattered dose rate values at the operator's eye level are reported for all acquisition modes available in different thicknesses of absorbent media and angiography. The characterization was performed according to the European DIMOND and SENTINEL protocols adapted to pediatric procedures. The air kerma at the entrance surface (ESAK) was measured and the image quality parameters signal-to-noise ratio (SNR) and a figure of merit (FOM) were calculated. The scattered dose rate was measured in personal dose equivalent units. The ESAK for fluoroscopic modes ranged from 0.2 to 35.6 μGy/image when passing from 4 to 20 cm of polymethyl methacrylate (PMMA). For the cine mode, these values ranged from 2.8 to 160.1 μGy/image. The values of the image quality parameters showed a correct system configuration, although abnormal values were observed in the medium fluoroscopic mode. As for the scattered dose rate at the level of the cardiologist's eyes, the highest value is PMMA with a thickness of 20 cm, where the cine mode reached 9.41 mSv·h-1. The differences found from previous evaluations can be explained by the deterioration of the system and the change of one of the X-ray tubes.

Keywords: Image Quality; Interventional Cardiology; Personal Equivalent Dose; ESAK; Radiation

ARTICLE INFO

Received: 6 May 2019
Accepted: 9 July 2019
Available online: 18 July 2019

1. Introduction

Medical applications currently represent the main source of artificial exposure of the world's population to ionizing radiation, particularly computed tomography and interventional radiology procedures[1]. According to the US National Council on Radiation Protection and Measurements, interventional radiology procedures were identified as the third largest contributor to collective dose (average dose to a population), after computed tomography and nuclear medicine[2].

Every interventional cardiology procedure involves a risk to the health of patients, operators and the general public. The primary objective of radiation protection is to provide an appropriate standard of protection for people and the environment, without unduly limiting these practices. The three fundamental principles of radiation protection are justification, optimization and the application of dose limits. For the patient, the first two principles are used, highlighting within optimization the definition of diagnostic reference levels. For personnel and the general public, the use of dose limits is the essential tool for avoiding

deterministic effects and minimizing the occurrence of stochastic effects[3].

It has been reported that children are more sensitive to ionizing radiation because they have a longer life expectancy[4]. As a result, they are at greater risk of developing and manifesting the harmful effects of ionizing radiation. This greater radiosensitivity is due to the fact that their cells have a high mitotic index and many of them are not yet differentiated, which means that their genetic material can be exposed for a longer time to ionizing radiation[5].

In the case of medical personnel, it is known that eye exposure can cause lens opacity[6] due to the co-aggregation of lens proteins by ionizing radiation. Haskal[7] demonstrated radiation-induced cataracts in 8% of 59 interventional radiologists attending a scientific meeting in New York. In addition, studies conducted by the International Atomic Energy Agency (IAEA), called "Retrospective Evaluation of Lens Lesions and Dose"[8] and initiated since 2008, obtained data on the high percentage of lens opacities in medical personnel when radiation protection tools were not used[9,10]. With this and other antecedents, in April 2011 the International Commission on Radiological Protection (ICRP) published a statement announcing a reduction in the dose thresholds for this organ. For medical personnel, the ICRP now recommends a dose limit equivalent to the lens of the eye of 20 mSv in one year, averaged over a period of 5 years, without exceeding 50 mSv in one year[11,12].

To reduce the risks associated with ionizing radiation, both to patients and medical staff during fluoroscopic X-ray procedures, adequate training in protection and the implementation of Quality Assurance programs are recommended[13,14].

X-ray systems used in pediatric interventional procedures are complex to evaluate, due to the different models and technologies available on the market, as well as their multiple configuration options and acquisition modes. Sometimes, medical specialists do not have standard criteria to compare the advantages and disadvantages among the available technologies, nor to select which is the best option among the different acquisition modes. Thus, the characterization or evaluation of these systems in terms of dose and image quality using test objects offers a wide range of useful data to understand the characteristics of angiographs, allowing the selection of the most appropriate protocols and acquisition modes for different procedures and patient sizes.

Therefore, this paper presents the optimized methodology and results of the new characterization performed in 2013 in terms of dose and image quality of the X-ray system used in the main pediatric hemodynamics service in Chile. In addition, the values of the scattered dose rate at the level of the eyes of the operators in different thicknesses of absorbent medium and in all acquisition modes available in the equipment are presented.

2. Material and method

A Siemens Axiom Artis BC biplane angiograph equipped with image intensifier (Siemens AG, Germany) belonging to the Department of Hemodynamics of the Hospital Dr. Luis Calvo MacKenna, Santiago, Chile, was characterized. The angiograph was equipped with a 100 kW generator at 100 kV, installed in 2006 and adapted for pediatric procedures, with an anti-diffusing grating (Siemens 05660217) with a 17:1 grating ratio, 70 lines/cm, and 100 cm focal distance. In 2012, the vertical C-arc X-ray tube was changed. The image intensifiers had a maximum diameter of 33 cm and allow three field sizes (33, 22, and 17 cm). The system was configured by the local Siemens service with three examination protocols (newborn, infant and child), three fluoroscopy modes (low (FL), medium (FM) and high dose (FH)) with 15 images (pulses)/s, and a single acquisition mode or cine (CI) with 30 images/s. In addition, filters from 0.1 to 0.9 mm Cu and virtual collimation were also available. The distance from the floor to the isocenter was 107 cm and the isocenter focus distance was 76 cm.

The methodology for this type of evaluation has been developed in the framework of research programs of the European Commission, such as: "Dose and image quality in digital imaging and interventional radiology"[15] and "Safety and efficacy for new imaging techniques using new equipment to support European legislation" (SENTINEL)[16]. Since 2008, Chile has been working to optimize this

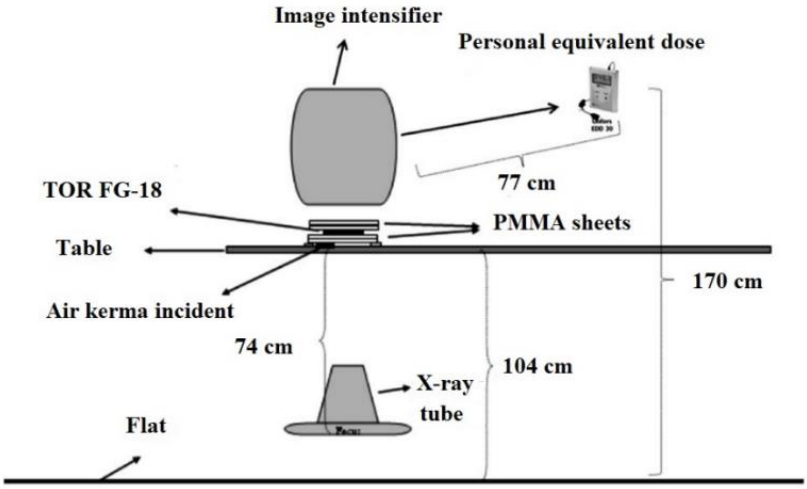

Figure 1. Schematic with details of the characterization and measurements of the scattered dose.

proposal through a series of publications[17-20].

Measurements were performed using 25 × 25 × 1 cm polymethylmethacrylate (PMMA) sheets, constructing thicknesses of 4, 8, 12, 16 and 20 cm. The ratio between the PMMA and patient chest can be considered as –1.5[21]. An Unfors Xi solid detector (model 8201010-A) with a measuring probe was used to determine the dose rate at the entrance and an Unfors EED-30 system (model 8131010-C) was used to measure the scattered dose rate at the cardiologist's position. Both instruments were calibrated at Unfors RaySafe laboratories in 2013.

A Leeds TOR 18-FG test object (Leeds Test Objects Inc., Boroughbridge, UK) was used to evaluate aspects of image quality. The object contains a set of 14 groups of line pairs for high contrast spatial resolution (with a limit of 5 lines pairs/mm) and 18 circles (11 mm diameter) for low contrast threshold evaluation. This test object is designed to provide a continuous verification of imaging performance in fluoroscopic systems. The test object was positioned at the isocenter and at the center of the PMMA thickness during all measurements.

2.1 Dosage at entry

The dosimetric magnitude measured in contact with the PMMA thickeners was the incident air kerma (IAK), however, to facilitate the comparison of our results these values were expressed in terms of air kerma at the entrance surface (ESAK), for which the IAK values were multiplied by the backscatter factor of 1.3[22].

For a thickness of 4 cm of PMMA and with the test object at the isocenter, the distance from the table (measured from its top face) to the ground was 104 cm. The distance from the table to the Unfors Xi detector was 1 cm. The distance from the table to the isocenter was 3 cm, and the distance from the focus to the X-ray detector (Unfors Xi) was 74 cm (**Figure 1**). For 8, 12, 16 and 20 cm of PMMA, this distance was reduced to 72, 70, 68 and 66, respectively, in order to keep the test object at the isocenter (the table was shifted down by 2 cm when 4 cm of PMMA was added). The image intensifier was always kept 5 cm from the top of the PMMA plates (also to simulate typical clinical working conditions).

Due to the numerous measurements performed (for 4, 8, 12, 16 and 20 cm PMMA) for all acquisition modes, a field size of 22 cm was used, and to avoid errors in dose estimations, the images of the test object were recorded simultaneously (**Figure 2**).

2.2 Image quality

The DICOM images obtained were stored in 1024 × 1024 pixels and 8-bit format (fluoroscopy series) and 512 × 512 pixels and 8-bit format (cine series) on the workstation of the X-ray system and recorded on CD-ROMs for further analysis. The images were evaluated using Osiris version 4.18 software. Image quality was evaluated by analyzing the low contrast circles in images 10, 12 and 15 of each saved series. **Figure 2** shows the selection of

the ROIs (rectangular) for numerical analysis, through the following parameters[18,19]:

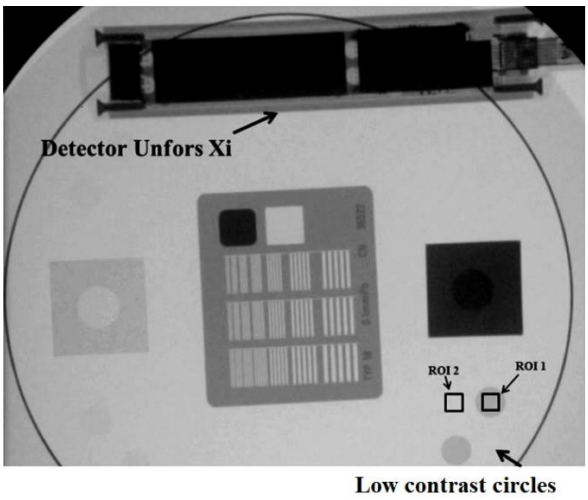

Figure 2. Example of one of the images of the test object used for numerical quality assessment. The image corresponds to cine mode, FOV 22 cm and 8 cm of PMMA.

Signal-to-noise ratio:

$$SNR = \frac{[BG\text{-}ROI]}{\sqrt{\frac{(SD_{ROI}^2 + SD_{BG}^2)}{2}}} \quad (1)$$

where BG: background value, the mean value of the pixel content in the rectangular region of interest near the low-contrast circle number 1 (ROI 2); ROI: mean value of the pixel content in the selected region of interest inside the circle number 1 (ROI 1); SD_{ROI} and SD_{BG}: standard deviation for ROI and BG (**Figure 2**), and

(2) Figure of merit:

$$FOM_1 = \frac{SNR^2}{ESAK} \quad (2)$$

where ESAK: kerma air at the entrance surface, at the point where the X-ray beam axis is incident on the PMMA.

2.3 Dose dispersed to the operator

The operational magnitude measured as scattered dose in the simulated position of the cardiologist's eyes was the personal equivalent dose Hp (10), which is an estimate of the equivalent dose in soft tissue at a depth of 10 mm[22]. These measurements were performed without any type of radiological protection element, thus simulating the maximum irradiation conditions for the personnel. The Unfors EED-30 detector (model 8131010-C) was positioned 0.77 m from the isocenter and 1.7 m from the floor (**Figure 1**). It should be noted that these measurements were carried out in conjunction with the determination of the PMMA incoming dose rate and the evaluation of image quality.

Table 1. Kerma air at the inlet surface (ESAK) per image, number of images, additional filter, tube potential and tube current for the different acquisition modes, examination protocols and all PMMA thicknesses

Mode of acquisition	Protocol of examination	PMMA (cm)	ESAK (mGy/min)	N° images	ESAK µGy/images)	Tube potential (kVp)	Tube current (mA)	Filter (mmCu)
FL	Newborn		0.11		0.2	71.5	18.0	0.9
FM	Newborn		0.18		0.3	77.0	18.3	0.9
FH	Newborn		0.23		0.4	58.0	79.4	0.9
CI	Newborn		5.08		2.8	52.7	98.6	0.2
FL	Infant		0.23		0.4	77.0	26.7	0.9
FM	Infant		0.40		0.7	77.0	26.7	0.9
FH	Infant		0.91		1.5	58.0	79.4	0.9
CI	Infant		13.54		7.5	52.7	98.6	0.3
FL	Child		0.47		0.8	77.0	30.6	0.9
FM	Child		0.90		1.5	77.0	39.0	0.9
FH	Child		2.06		3.4	66.0	80.9	0.6
CI	Child		19.29		10.7	61.0	230	0.6
FL	Child		1.23		2.1	70.0	44.9	0.9
FM	Child		2.40		4.0	77.0	57.5	0.9
FH	Child		5.48		9.1	66.0	142.6	0.6
CI	Child		57.54		32.0	76.6	346.1	0.3
FL	Child		3.89		6.5	77.0	69.5	0.9
FM	Child		6.51		10.9	77.0	88.8	0.9
FH	Child		21.35		35.6	68.0	161.7	0.3
CI	Child		288.13		160.1	85.0	327.3	0.0

3. Results

Table 1 shows the ESAK values for the different acquisition modes, available proto-colors, PMMA thicknesses and number of images per second. In addition, the exposure factors for each of the conditions and their respective added filters are shown.

Figures 3 and **4** show the values achieved for the numerical parameters SNR and FOM for the different acquisition modes of the equipment and PMMA thicknesses.

Figure 5 illustrates the personal dose equivalent values expressed in units of $mSv \cdot h^{-1}$ for the different equipment acquisition modes and PMMA thicknesses.

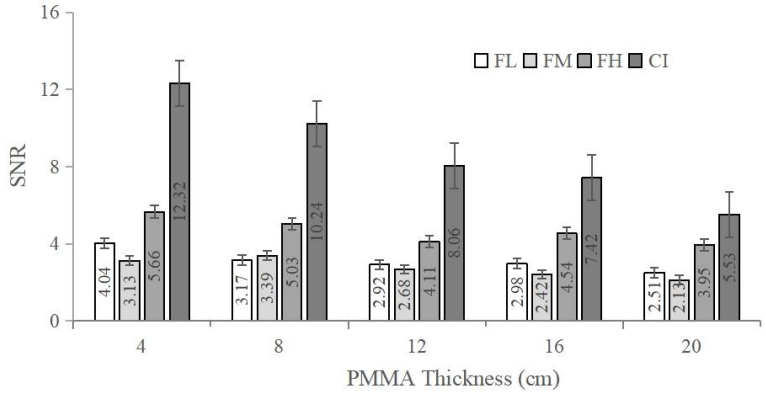

Figure 3. Signal-to-noise ratio (SNR) values for the different simulated patient thicknesses and operating modes (low (FL), medium (FM), high (FH) and cine (CI) fluoroscopy). Field size: 22 cm.

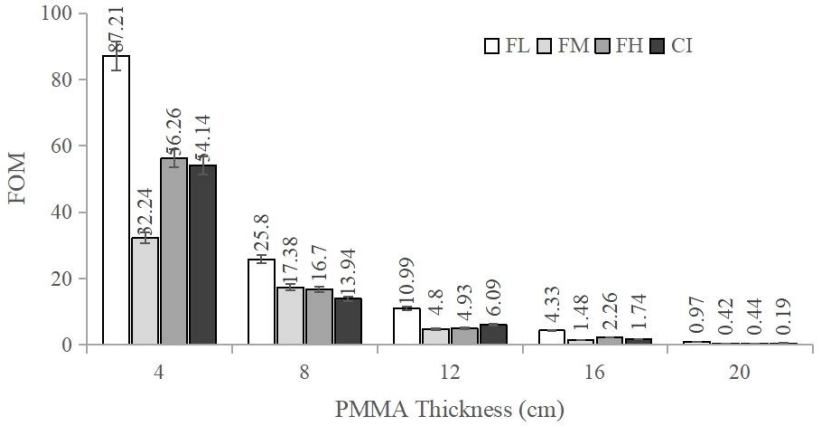

Figure 4. Figure of merit (FOM) values for the different simulated patient thicknesses and operating modes (low fluoroscopy (FL), medium (FM), high (FH) and cine (CI)). Field size: 22 cm.

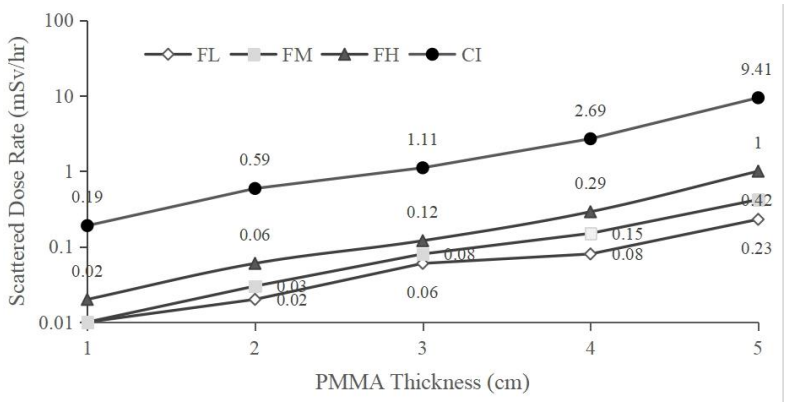

Figure 5. Scattered dose values (personal equivalent dose) at the position of the cardiologist's eyes for the different simulated patient thicknesses and operating modes (low fluoroscopy (FL), medium (FM), high (FH) and cine (CI)). Field size: 22 cm.

4. Discussion

In Latin America and the Caribbean, pediatric interventional cardiology procedures are performed by pediatric cardiology specialists, who in some cases do not have specific training in radiological imaging and radiological protection. In addition, quality controls are not carried out on a permanent basis, nor are quality assurance programs implemented, according to IAEA data for the region[23].

The IAEA, aware of this situation in Latin America and the Caribbean, has implemented two technical cooperation projects entitled "Radiological protection of patients during medical examinations (TSA3), RLA/9/057"[24] and "Ensuring radiological protection of patients during medical examinations (TSA3), RLA/9/067"[25]. In both projects, Chile has led the study in the fields of dose and image quality characterization of X-ray systems[18-20,26-28] , as well as dosimetry and radiological protection for pediatric patients[23,29] and medical personnel[9,20-32] involved in interventional cardiology procedures, which is why it is being considered as a model for extending its experience to other countries.

In Ubeda *et al.*[33], these works and future challenges are discussed in detail, highlighting the importance of permanently evaluating X-ray systems in terms of dose and image quality, as well as the levels of different radiation to which medical personnel are exposed. To achieve this, it becomes urgent to review our legal framework in the field of radiation safety.

4.1 Dose at PMMA inlet

The ESAK for FL acquisition mode ranged from 0.2 to 6.5 µGy/image, when the PMMA thickness was increased from 4 to 20 cm. For the FM acquisition mode, the ESAK ranged from 0.3 to 10.9 µGy/image, for the same PMMA thicknesses. For the FH acquisition mode, the ESAK values varied between 0.4 and 35.6 µGy/image. For the CI acquisition mode, the range was between 2.8 and 160.1 µGy/image (**Table 1**).

In general, these dose values were similar to those described in previous works where this system was evaluated[18,19], which demonstrates a constancy over time despite having changed the X-ray tube a few months before this characterization.

It is also relevant to indicate that the increase in the dose at the PMMA entrance due to the size in our simulated patients was between 50 and 60 times for the fluoroscopy and cine modes, respectively. Finally, it should be noted that the dose savings that can be generated for the patient, if the lower dose fluoroscopic (FL) mode is used instead of the IC mode for archiving our examinations, would be 13 to 25 times.

4.2 Image quality

The numerical parameter SNR should be higher when changing from the lower dose mode (FL) to the higher dose mode (CI) in all PMMA thicknesses analyzed, a situation that, according to **Figure 3**, occurs for all acquisition modes, except for the intermediate fluoroscopic dose mode (FM), a situation that is confirmed in **Figure 5**. This is an indication that this fluoroscopic acquisition mode needs to be reviewed and adjusted by the technical service, as was done in 2008[18]. Another variable to consider in this analysis is the influence of the patient's thickness and how the X-ray system as a whole, through the auto-automatic exposure control, adjusts the parameters of potential, tube current and copper filters (**Table 1**). In comparison with the work done in 2008[18], the SNR values for the IC mode decreased steadily with the increase of PMMA thickness.

According to **Figure 5**, it is highly recommended to use the FL mode over the other options, since it provides the highest FOM values. The FOM parameter has been used by other auto-res[34,35]; to optimize signal detectability in digital images. This parameter makes it possible to relate image quality and the dose required to obtain that image, which gives an objective indication of the cost/benefit ratio for the patient when exposed to radiation.

4.3 Dose dispersed to the operator

Figure 5 shows the scattered dose rate measured with the X-ray tube in the vertical location of the C-arc, in the usual position of the cardiologist's eyes, unprotected for the three fluoroscopic modes and for cine mode. The figure also shows the varia-

tion of the dispersed dose rate for the different examination protocols. As expected, the highest values were for the 20 cm thickness of PMMA, where the CI mode was equal to 9.41 $mSv \cdot h^{-1}$. In the case of FL mode, its dose rate was 41 times lower.

5. Conclusion

The main X-ray system used exclusively for pediatric interventional cardiology procedures in Chile was again characterized in terms of dose and image quality. In addition, the levels of scattered radiation in the simulated position of the cardiologist's eyes were evaluated. The results achieved in these evaluations were relatively similar to those obtained previously; however, the inherent deterioration of the system as a whole, as well as the change of the vertical C-arc X-ray tube, may partly explain the variations.

Finally, it is urgent to update the Chilean legal framework so that this type of procedure becomes mandatory.

References

1. UNSCEAR. UNSCEAR 2008 Report: Sources and Effects of Ionizing Radiation. Vienna International Centre: United Nations Scientific Committee on Effects of Atomic Radiations; 2008.
2. NCRP. Ionizing radiation exposure of the population of the United States. Report No. 160. Bethesda: National Council on Radiation Protection and Measurements; 2009.
3. ICRP. The 2007 recommendations of the international commission on radiological protection. Publication 103. Annals of the ICRP 2007; 37: 332.
4. Board on Radiation Effects Research (BEIR). Health risks from exposure to low levels of ionizing radiation: BEIR VII phase 2. Washington DC: National Academies Press; 2006. p. 424.
5. Hall E, Giaccia A. Radiobiology for the radiologist. New York: Lippincott Williams and Wilkins; 2006. p. 16–29, 135–155, 216.
6. Vano E, Gonzalez L, Beneytez F, *et al*. Lens injuries induced by occupational exposure in non-optimized interventional radiology laboratories. The British Journal of Radiology 1998; 71(847): 728–733.
7. Haskal ZJ. Interventional radiology carries occupational risk for cataracts. RSNA News 2004; 14: 5–6.
8. RELID. Retrospective evaluation of lens injuries and dose. Vienna, Austria: International Atomic Energy Agency; 2014.
9. Ubeda C, Vano E, Gonzalez L, *et al*. Scatter and staff dose levels in paediatric interventional cardiology: A multicentre study. Radiation Protection Dosimetry 2010; 140(1): 67–74.
10. Ciraj-Bjelac O, Rehani MM, Sim KH, *et al*. Risk for radiation-induced cataract for staff in interventional cardiology: Is there reason for concern? Catheterization and Cardiovascular Interventions 2010; 76(6): 826–834.
11. ICRP. Statement on tissue reactions. Ottawa: International Commission on Radiological Protection; 2011.
12. Rehani MM, Vano E, Ciraj-Bjelac O, *et al*. Radiation and cataract. Radiation Protection Dosimetry 2011; 147(1–2): 300–304.
13. EC. Directive 84/466/Euratom 30/06/1997 [Internet]. Luxembourg: European Commission; 1997. Available from: http://ec.eu-ropa.eu/energy/nuclear/radiopro-tection /doc/legislation/9743_en.pdf(Cons.01/2014).
14. IAEA. Radiation Protection and Radiation Source Safety: International Basic Safety Standards. Vienna: International Atomic Energy Agency; 2011.
15. DIMOND. Measures for optimising radiological information and dose in digital imaging and interventional radiology. Luxembourg: European Commission; 2002.
16. Faulkner K, Malone J, Vano E, *et al*. The SENTINEL project. Radiation Protection Dosimetry 2008; 129(1–3): 3–5.
17. Vano E, Ubeda C, Martinez L C, *et al*. Paediatric interventional cardiology: Flat detector versus image intensifier using a test object. Physics in Medicine & Biology 2010; 55(23): 7287–7297.
18. Vano E, Ubeda C, Leyton F, *et al*. Radiation dose and image quality for paediatric interventional cardiology. Physics in Medicine and Biology 2008; 53: 4049–4062.
19. Ubeda C, Vano E, Miranda P, *et al*. Radiation dose and image quality for paediatric interventional cardiology systems. Radiation Protection Dosimetry 2011a; 147: 429–438.
20. Ubeda C, Vano E, Miranda P, *et al*. Radiation dose and image quality for adult interventional cardiology in Chile: A national survey. Radiation Protection Dosimetry 2011b; 147(1–2): 90–93.
21. Rassow J, Schmaltz AA, Hentrich F, *et al*. Effective doses to patients from paediatric cardiac catheterization. The British Journal of Radiology 2000; 73(866): 172–183.
22. ICRU. Patient dosimetry for x-rays used in medical imaging. International Commission on Radiological Units and Measurements. Report 74. Journal of the ICRU 2005; 5: 113.
23. Vano E, Ubeda C, Miranda P, *et al*. Radiation protection in pediatric interventional cardiology: An IAEA PILOT program in Latin America. Health Physics 2011; 101(3): 233–237.
24. IAEA. Annual report for 2007. Vienna: International Atomic Energy Agency; 2007.
25. IAEA. Building partnerships to fight cancer. Vienna: International Atomic Energy Agency; 2009.
26. Vano E, Ubeda C, Fernandez J M, *et al*. Dose assessment during the commissioning of flat detector

imaging systems for cardiology. Radiation Protection Dosimetry 2009b; 136(1): 30–37.
27. Ubeda C, Vano E, Gonzalez L, *et al*. Influence of the anti-scatter grid on dose and image quality in pediatric interventional cardiology X-ray systems. Catheterization and Cardiovascular Interventions 2012; 82(1): 51–57.
28. Vano E, Ubeda C, Leyton F, *et al*. Radiation dose and image quality for paediatric interventional cardiology. Physics in Medicine and Biology 2008; 53: 4049–4062.
29. Ubeda C, Vano E, Miranda P, *et al*. Pilot program on patient dosimetry in pediatric interventional cardiology in Chile. Medical Physics 2012; 39(5): 2424–2430.
30. Vano E, Ubeda C, Leyton F, *et al*. Staff radiation doses in interventional cardiology: Correlation with patient exposure. Pediatric Cardiology 2009; 30(4): 409-413.
31. Ubeda C, Vano E, Gonzalez L, *et al*. Influence of the anti-scatter grid on dose and image quality in pediatric interventional cardiology X-ray systems. Catheterization and Cardiovascular Interventions 2013; 82(1): 51–57.
32. Vassileva J, Vano E, Ubeda C, *et al*. Impact of the X-ray system setting on patient dose and image quality; A case study with two interventional cardiology systems. Radiation Protection Dosimetry 2013; 155(3): 329–334.
33. Ubeda C, Vano E, Gonzalez L, *et al*. Evaluation of patient doses and lens radiation doses to interventional cardiologists in a nationwide survey in Chile. Radiation Protection Dosimetry 2013; 157(1): 36–43.
34. Zamenhof RG. The optimization of signal detectability in digital fluoroscopy. Medical Physics 1982; 9(5): 688–694.
35. Gagne RM, Boswell JS, Myers KJ. Signal detectability in digital radiography: Spatial domain figures of merit. Medical Physics 2003; 30(8): 2180–2193.